

Lithium Diisopropylamide-Mediated Enolizations: Solvent-Dependent Mixed Aggregation Effects

Xiufeng Sun and David B. Collum*

Contribution from the Department of Chemistry and Chemical Biology, Baker Laboratory, Cornell University, Ithaca, New York 14853-1301

Received June 17, 1999

Abstract: ^6Li and ^{15}N NMR spectroscopic investigations of lithium diisopropylamide-mediated ester enolization in THF, *t*-BuOMe, HMPA/THF, and DMPU/THF (HMPA = hexamethylphosphoramide, DMPU = 1,3-dimethyl-3,4,5,6-tetrahydro-2(1*H*)-pyrimidone) reveal substantial concentrations of mixed aggregates. While previous quantitative rate studies revealed that the metalations by lithium diisopropylamide (LDA) homonuclear dimers proceed at nearly solvent-independent rates, the reactivities of the intermediate mixed aggregates are markedly lower and quite sensitive to the choice of solvent. The autoinhibition correlates with the relative stabilities of the mixed aggregates. However, the relative stabilities do not correlate in a simple fashion with the ligating properties of the solvent.

Introduction

In the 1960s mixed aggregation effects on alkyllithium-mediated anionic polymerizations were clearly documented.¹ Beginning with a seminal review in 1984 followed by a second in 1988,² Seebach mounted a campaign to alert synthetic organic chemists to the possible consequences of aggregation and mixed aggregation on organolithium reactions.^{3a} There is now ample evidence, for example, that mixed aggregates of lithium amides form and influence their chemistry.^{3b} However, there are very few instances in which insights have been gleaned as to *how* these mixed aggregates influence reactivity.^{3–8}

(1) *Ions and Ion Pairs in Organic Reactions*; Szwarc, M., Ed.; Wiley: New York, 1972; Vols. 1 and 2. Szwarc, M. *Carbanions, Living Polymers, and Electron-Transfer Processes*; Interscience: New York, 1968. Morton, M. *Anionic Polymerization: Principles and Practice*; Academic Press: New York, 1983. *Anionic Polymerization: Kinetics, Mechanism, and Synthesis*; McGrath, J. E., Ed.; American Chemical Society: Washington, 1981. Cubbon, R. C. P.; Margerison, D. *Prog. React. Kinet.* **1965**, *3*, 403. Roovers, J. E. L.; Bywater, S. *Macromolecules* **1968**, *1*, 328.

(2) Seebach, D. *Angew. Chem., Int. Ed. Engl.* **1988**, *27*, 1624. Seebach, D. In *Proceedings of the Robert A. Welch Foundation Conferences on Chemistry and Biochemistry*; Wiley: New York, 1984.

(3) (a) For leading references to mixed aggregation effects in organolithium chemistry, see: Jackman, L. M.; Rakiewicz, E. F. *J. Am. Chem. Soc.* **1991**, *113*, 1202. Kremer, T.; Harder, S.; Junge, M.; Schleyer, P. v. R. *Organometallics* **1996**, *15*, 585. Thompson, A.; Corley, E. G.; Huntington, M. F.; Grabowski, E. J. J.; Remenar, J. F.; Collum, D. B. *J. Am. Chem. Soc.* **1998**, *120*, 2028. (b) For leading references to mixed aggregation effects in lithium amides, see: Romesberg, F. E.; Collum, D. B. *J. Am. Chem. Soc.* **1994**, *116*, 9198. (c) Remenar, J. F.; Collum, D. B. *J. Am. Chem. Soc.* **1997**, *119*, 5573. (d) Leung, S. S. W.; Streitwieser, A. *J. Org. Chem.* **1999**, *64*, 3390.

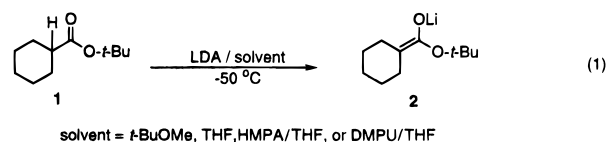
(4) Depue, J. S.; Collum, D. B. *J. Am. Chem. Soc.* **1988**, *110*, 5524.

(5) Majewski, M.; Nowak, P. *Tetrahedron Lett.* **1998**, *39*, 1661.

(6) Huisgen, R. In *Organometallic Chemistry*; Monograph Ser. No. 147 American Chemical Society: Washington, DC, 1960; pp 36–87.

(7) For crystal structures of lithium amide mixed aggregates, see: Williard, P. G.; Hintze, M. J. *J. Am. Chem. Soc.* **1987**, *109*, 5539. Mair, R. S.; Clegg, W.; O'Neil, P. A. *J. Am. Chem. Soc.* **1993**, *115*, 3388. Engelhardt, L. M.; Jacobsen, G. E.; White, A. H.; Raston, C. L. *Inorg. Chem.* **1991**, *30*, 3978. Williard, P. G.; Hintz, M. J. *J. Am. Chem. Soc.* **1990**, *112*, 8602. Zerges, W.; Marsch, M.; Harnes, K.; Boche, G. *Angew. Chem., Int. Ed. Engl.* **1989**, *28*, 1392. Clegg, W.; Greer, J. C.; Hayes, J. M.; Mair, F. S.; Noland, P. M.; O'Neil, P. A. *Inorg. Chim. Acta* **1997**, *258*, 1.

The preceding paper describes quantitative rate studies of the lithium diisopropylamide-mediated ester enolization (eq 1).^{9,10}



By carrying out the reactions under pseudo-first-order conditions with the ester maintained at low concentrations so as to eliminate the effects of mixed aggregation, we showed that the nearly solvent-independent metalation rates in four very different solvents (*t*-BuOMe, THF, HMPA/THF, and DMPU/THF) belie highly solvent-dependent changes in mechanism. However, under more standard conditions employed in preparative organic chemistry, the LDA and ester would be used in nearly equimolar proportions. During the course of such enolizations, lithium enolates are generated while the lithium diisopropylamide (LDA) is consumed; the conditions change continuously as a function of percent conversion. If LDA–lithium enolate mixed aggregates form to an appreciable extent along the reaction coordinate they will *necessarily* influence reactivity.

This paper outlines investigations of the LDA-mediated enolization of ester **1** under conditions that optimize the influence of mixed aggregates. Using primarily ^6Li and ^{15}N NMR spectroscopy, we will show that intervening mixed aggregates retard the rates of enolization in all solvents. The onset and degree of autoinhibition correlates qualitatively with the formation and relative stability of intervening mixed

(8) Collum, D. B. *Acc. Chem. Res.* **1993**, *26*, 227. For other reviews of lithium amide structural investigations, see: (a) Gregory, K.; Schleyer, P. v. R.; Snaith, R. *Adv. Inorg. Chem.* **1991**, *37*, 47. (b) Mulvey, R. E. *Chem. Soc. Rev.* **1991**, *20*, 167. Beswick, M. A.; Wright, D. S. In *Comprehensive Organometallic Chemistry II*; Abels, F. W., Stone, F. G. A., Wilkinson, G., Eds.; Pergamon: New York, 1994; Vol. 1, Chapter 1.

(9) Sun, X.; Collum, D. B. *J. Am. Chem. Soc.* **2000**, *122*, 2452–2458.

(10) Sun, X.; Kenkre, S. L.; Remenar, J. F.; Gilchrist, J. H.; Collum, D. B. *J. Am. Chem. Soc.* **1997**, *119*, 4765.

Table 1. ^6Li and ^{15}N NMR Spectral Data^{a,b}

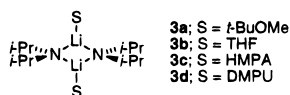
compd	^6Li , δ (m, J_{LiN})	^{15}N , δ (m, J_{LiN})
2a	0.38, 0.35, 0.28, 0.12, 0.01 ^c	
3a	1.87 (t, 5.0)	70.2 (q, 5.0)
7a	1.36 (d, 5.3)	73.1 (q, 5.3)
8a^d	2.55 (t, 4.8) 1.65 (–) ^e	70.5 (br m)
9a	2.08 (t, 4.5) 1.34 (d, 6.4)	71.1 (q, 5.2)
2b	–0.29 (s) ^e	
3b	1.91 (t, 5.0)	74.7 (q, 5.0)
7b	0.83 (d, 5.1)	76.3 (q, 5.1)
2c	–0.04, –0.25, –0.50, –0.57 ^c	
3c	1.60 (t, 5.0)	74.3 (q, 5.2)
7c	0.93 (d, 5.1)	76.9 (q, 4.7)
2d	–0.35 (s) ^e	
3d	1.88 (t, 4.9)	73.3 (q, 4.7)
7d	0.90 (d, 5.1)	75.3 (q, 5.1)
4	2.08 (t, 4.4) 1.71 (t, 5.3)	71.1 (q, 4.9)
5	1.74 (t, 5.0), 1.19 (d, 5.4), 1.00 (d, 6.7) ^f	79.2 (br q, 5.7) 77.6 (q, 5.5)

^a Samples in *t*-BuOMe were recorded at –60 °C. All others were determined at –90 °C. ^b Spectra were recorded on samples containing 0.13 M total lithium concentration (normality). Coupling constants were measured after resolution enhancement. Multiplicities are denoted as follows: s = singlet, d = doublet, t = triplet, q = quintet, br mult = broad multiplet. The chemical shifts are reported relative to 0.3 M $^6\text{LiCl}/\text{MeOH}$ at –100 °C (0.0 ppm) and neat Me_2NEt (25.7 ppm). All J values are reported in hertz. ^c All signals attributed to homonuclear enolate aggregates (**2a–d**) are singlets. ^d Recorded at –125 °C. ^e Obscured by another resonance. ^f This resonance is very sensitive to the [DMPU].

aggregates. However, the relative propensities to form mixed aggregates do *not* correlate with the coordinating power of the solvents.

Results

LDA Solution Structures. Previous investigations have shown that LDA is a disolvated dimer (**3a** and **3b**) in ethereal solvents.⁸ Moreover, HMPA quantitatively displaces THF from dimer **3b** to afford dimer **3c** without detectable deaggregation.¹¹ To complete the structural foundations, we investigated LDA in DMPU/THF solutions using a combination of NMR and IR spectroscopies. The spectra are archived in the Supporting Information.



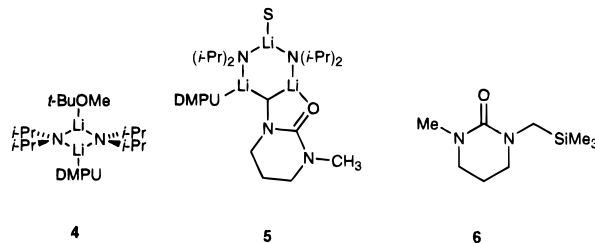
IR spectra recorded on 0.1 M solutions of LDA in THF containing 2.0 equiv of DMPU per Li clearly show carbonyl absorbances at 1658 and 1636 cm^{-1} corresponding to free and bound DMPU (respectively).^{9,12} The results are fully consistent with the formation of DMPU-solvated dimer **3d**. ^6Li and ^{15}N NMR spectra recorded on 0.1 M solutions of [^6Li , ^{15}N]LDA¹³ in DMPU/THF (1.0–10 equiv) contain exclusively a ^6Li triplet and ^{15}N quintet anticipated for cyclic dimer **3d** (Table 1). Addition of <1.0 equiv failed to show two discrete ^6Li resonances expected for mixed solvate at –120 °C, indicating that the free and LDA-bound DMPU are in rapid exchange on the NMR time scales. While distinct free and lithium amide-

(11) Romesberg, F. E.; Gilchrist, J. H.; Harrison, A. T.; Fuller, D. J.; Collum, D. B. *J. Am. Chem. Soc.* **1991**, *113*, 5751.

(12) Aitken, C. T.; Onyszczuk, M. *J. Organomet. Chem.* **1985**, *295*, 149.

(13) Kim, Y.-J.; Bernstein, M. P.; Galiano-Roth, A. S.; Romesberg, F. E.; Williard, P. G.; Fuller, D. J.; Harrison, A. T.; Collum, D. B. *J. Org. Chem.* **1991**, *56*, 4435.

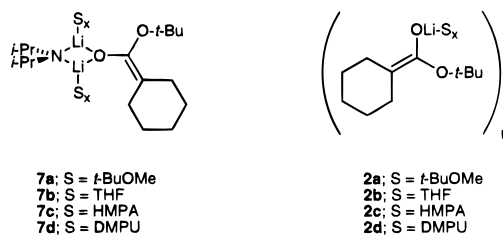
bound ligands have been observed on a number of occasions,¹⁴ strongly coordinating ethereal cosolvents such as THF can catalyze the exchange of other ligands via an associative process.¹⁴ Indeed, ^6Li and ^{15}N NMR spectra recorded on 0.1 M solutions of [^6Li , ^{15}N]LDA containing 0.5 equiv of DMPU in the poorly coordinating *t*-BuOMe¹¹ reveal mixed solvate **4** along with dimers **3a** and **3d** (Table 1). Mixed solvate **4** displays two distinct ^6Li resonances coupled¹⁵ to a single ^{15}N resonance.¹⁶



As an aside, solutions of [^6Li , ^{15}N]LDA in DMPU/THF aged at 0 °C slowly form a new species over several hours believed to be mixed aggregate **5** containing the dipole-stabilized¹⁷ anion of DMPU.¹⁸ The atomic connectivity of **5** was confirmed by single frequency decouplings¹⁵ of the three ^6Li resonances (1:1:1) and two ^{15}N resonances (1:1). Treatment of the solution containing putative mixed aggregate **5** with TMSCl affords the silylated DMPU derivative **6** as shown by comparison with a sample prepared independently using *s*-BuLi.¹⁹ DMPU metalation does not occur detectably under the conditions of the ester enolizations.

Structures of LDA/Lithium Enolate Mixed Aggregates.

Analyses of [^6Li , ^{15}N]LDA (0.1 M) with 1.0 equiv of ester **1-d**²⁰ at –90 °C in THF, HMPA/THF, and DMPU/THF reveal exclusively LDA dimers **3b–d**.²¹ Warming the samples periodically to –50 °C and cooling back down to –90 °C reveals mixed dimers **7b–d**, each displaying a characteristic ^6Li doublet and ^{15}N quintet (Table 1); spectra are archived in the Supporting Information. As the enolizations proceed to completion, uncharacterized enolates (**2a–d**) appear at the expense of the mixed dimers.²²



t-BuOMe affords somewhat different behavior. FT-IR studies⁹ show that mixtures of LDA and ester **1** contain both the dimer

(14) Hilmersson, G.; Davidsson, O. *J. Org. Chem.* **1995**, *60*, 7660. Hilmersson, G.; Ahlberg, P.; Davidsson, O. *J. Am. Chem. Soc.* **1996**, *118*, 3539. Hilmersson, G.; Arvidsson, P. I.; Davidsson, O. *J. Am. Chem. Soc.* **1996**, *118*, 3539. Lucht, B. L.; Collum, D. B. *J. Am. Chem. Soc.* **1996**, *118*, 2217. Lucht, B. L.; Collum, D. B. *J. Am. Chem. Soc.* **1994**, *116*, 6009. Lucht, B. L.; Bernstein, M. P.; Remenar, J. F.; Collum, D. B. *J. Am. Chem. Soc.* **1996**, *118*, 10707. Also, see ref 26.

(15) Gilchrist, J. H.; Harrison, A. T.; Fuller, D. J.; Collum, D. B. *J. Am. Chem. Soc.* **1990**, *112*, 4069.

(16) Addition of ≥ 1.0 equiv of DMPU to LDA in *t*-BuOMe afforded a precipitate.

(17) Beak, P. *Chem. Rev.* **1984**, *84*, 471. Beak, P.; Basu, D.; Gallagher, D. J.; Park, Y. S. *Acc. Chem. Res.* **1996**, *29*, 552.

(18) The base-mediated decomposition of DMPU was noted previously: Mukhopadhyay, T.; Seebach, D. *Helv. Chim. Acta* **1982**, *65*, 385.

(19) A sample of **6** was prepared independently by treatment of DMPU with *s*-BuLi at –78 °C followed by Me_3SiCl .

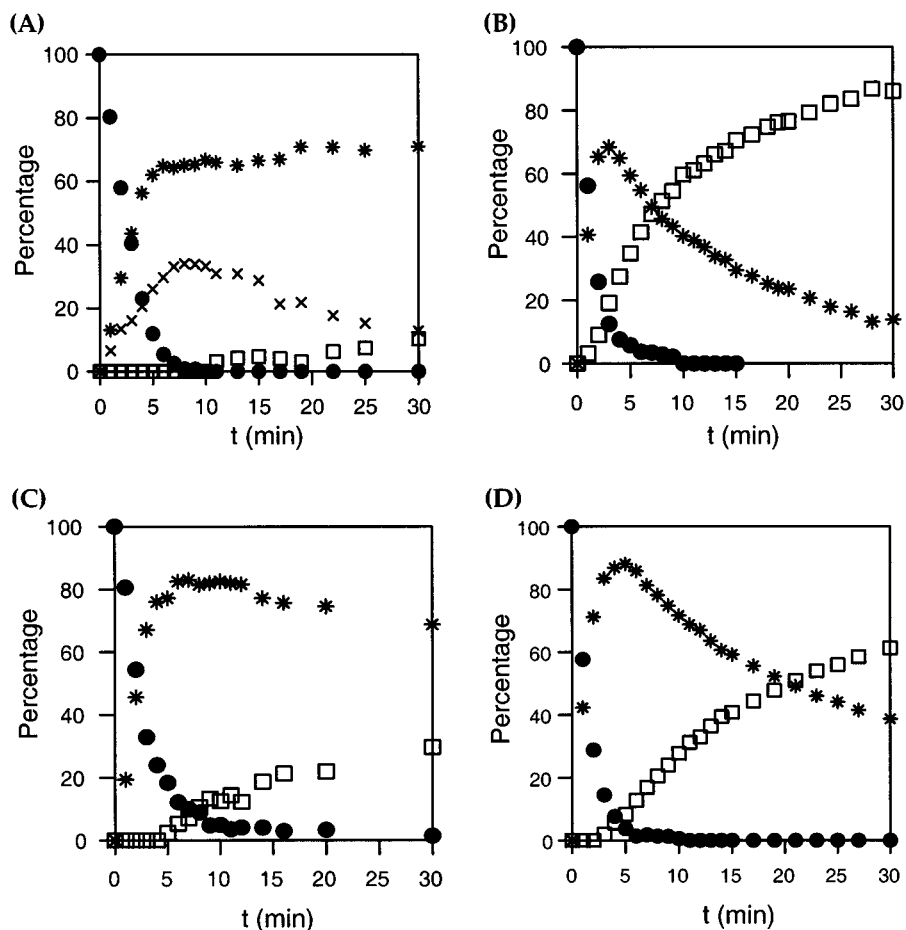


Figure 1. Concentrations of species vs time for the reaction of 0.1 M $[\text{}^6\text{Li}]\text{LDA}$ with 0.1 M ester **1-d₁** at $-50\text{ }^\circ\text{C}$ (as indicated by the percentage of integration in the ${}^6\text{Li}$ NMR spectra). Legend: ● represents LDA dimers (**3a-d**); * represents LDA-enolate mixed dimers (**7a-d**); □ represents homonuclear enolate aggregates (**2a-d**); × represents mixed trimer (**9a**). (A) Neat *t*-BuOMe; (B) neat THF; (C) 0.2 M HMPA in THF; and (D) 0.2 M DMPU in THF.

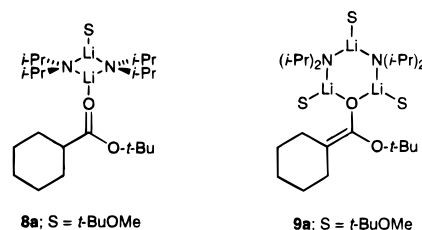
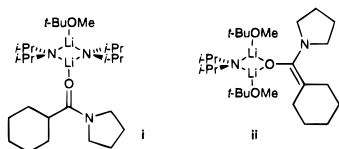
3a and an ester-LDA complex (**8a**). NMR spectroscopic analysis on analogous solutions of ester **1** and $[\text{}^6\text{Li}, \text{}^{15}\text{N}]\text{LDA}$ in *t*-BuOMe reveal LDA dimer **3a** along with precomplex **8a**. The appearance of two distinct ${}^6\text{Li}$ resonances and one ${}^{15}\text{N}$ resonance of **8a** at $-125\text{ }^\circ\text{C}$ confirms that the ligands are in the slow exchange limit. Warming of the samples to $-50\text{ }^\circ\text{C}$ affords predominantly mixed trimer **9a** at low conversion, mixed dimer **7a** at intermediate conversion, and several homonuclear enolate aggregates (**2a**) at full conversion. Trimer **9a** is characterized by a ${}^6\text{Li}$ doublet and ${}^6\text{Li}$ triplet (2:1) coupled to a single ${}^{15}\text{N}$ broad quintet (Table 1). Mixed dimer **7a** displays a ${}^6\text{Li}$ doublet and ${}^{15}\text{N}$ quintet.²³

(20) The rate measurements using LDA/HMPA mixtures employed **1-d₁** to allow the rates to be monitored at temperatures that maximized the solubility of HMPA.

(21) Traces of trimer **9 (9b; S = THF)** could be detected.

(22) Structural studies of enolates: Williard, P. G. In *Comprehensive Organic Synthesis*; Pergamon: New York, 1991; Vol 1, p 1. Setzer, W. N.; Schleyer, P. v. R. *Adv. Organomet. Chem.* **1985**, *24*, 353. Abbotto, A.; Leung, S. S.-W.; Streitwieser, A.; Kilway, K. V. *J. Am. Chem. Soc.* **1998**, *120*, 10807. Jackman, L. M.; Chen, X. *J. Am. Chem. Soc.* **1992**, *114*, 403.

(23) As part of our rate studies,⁹ we required the characterization of carboxamide precomplex **i** and mixed dimer **ii**. These spectra are archived in the Supporting Information.



Solvent-Dependent Rates. Monitoring solutions of $[\text{}^6\text{Li}]\text{LDA}$ and ester **1** at $-50 \pm 1\text{ }^\circ\text{C}$ in each of the four solvents provides insights into the degree of mixed aggregation and the consequences of mixed aggregation on the metalation rate. Figure 1 shows the time-dependent concentrations of LDA dimers (**3a-d**), mixed dimers (**7a-d**), mixed trimer (**9a**), and lithium enolates (**2a-d**). *x*-axes common to all plots (0–30 min) are employed to optimize direct comparisons; plots showing reaction to full conversion are included in the Supporting Information. In the discussion section, we will focus upon three facets of these plots: (1) the approach to the first few percent conversion in which the LDA is rapidly consumed and the mixed aggregates begin to appear, (2) the concentrations of all species as the mixed aggregates attain maximal concentrations, and (3) the time-dependent loss of the mixed aggregates and formation of homonuclear enolate aggregates.

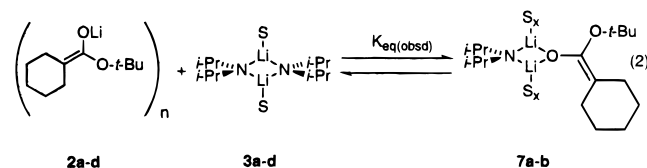
We can crudely²⁴ quantitate the extent of mixed aggregation by measuring the concentrations of the homonuclear and mixed aggregates when mixed dimers reach maximum concentrations

Table 2. Proportions of Homonuclear and Mixed Aggregates (Eq 2)^a

solvent	2:3:7	$K_{\text{eq(obsd)}}^b$
<i>t</i> -BuOMe	<1: <1: >99 ^c	> 10 ⁴
THF	19:13:68	18
DMPU/THF	8:4:88	240
HMPA/THF	7:10:83	98

^a Ratios derive by monitoring ester **1** (0.1 M) and [⁶Li]LDA (0.1 M) at -50 °C by ⁶Li NMR spectroscopy. The ratios are measured at the maximum concentration of mixed dimer ($[7]_{\text{max}}$). At these temperatures the resonances of the enolate aggregates (cf. Table 1) appear as only one singlet, except for *t*-BuOMe in which several resonances are summed. ^b $K_{\text{eq(obsd)}}$ is loosely²⁴ defined by eq 2. ^c Although trimer **9a** complicates the analysis, at no point do homonuclear aggregates **2a** and **3a** coexist.

($[7]_{\text{max}}$) and calculating $K_{\text{eq(obsd)}}$ (eq 2, Table 2). Thus, mixed



aggregates form to a limited extent in THF as evidenced by the coexistence of considerable concentrations of all three structural forms. They form to a substantially greater degree in DMPU/THF and in THF containing 1.0 equiv of HMPA. Metalations using LDA in *t*-BuOMe are somewhat more complex due to the existence of both mixed dimers and trimers. However, it is quite clear that the homonuclear lithium enolate aggregate and LDA dimer do not measurably coexist, indicating an *exceptional* relative stabilization of mixed aggregates. Overall, the promotion of mixed aggregates and the accompanying reduction of the LDA dimer concentrations maintains the following order: *t*-BuOMe > DMPU/THF > HMPA/THF > THF. This is central to the points made in the Discussion.

Discussion

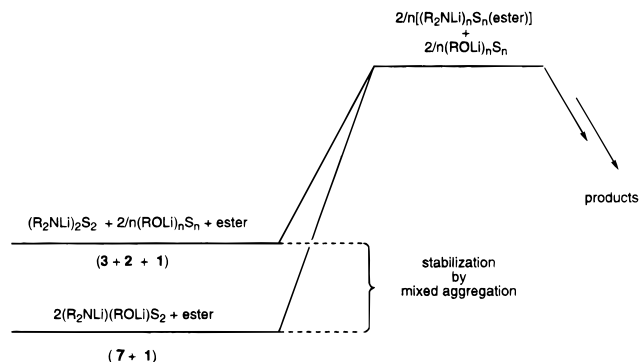
Previous studies of LDA and LiTMP revealed that enolates readily form mixed dimers and trimers with lithium amides.^{3a} While one could imagine that strongly coordinating solvents might retard mixed aggregate formation, the relationship of solvation and mixed aggregation is not that simple. Strong ligands such as HMPA seem to either promote or retard mixed aggregation of LDA or LiTMP, depending upon the precise choice of LiX salt.^{3a} In contrast, lithium hexamethyldisilazide (LiHMDS) forms mixed dimers and trimers with enolates only in poorly coordinating solvents such as *t*-BuOMe or hydrocarbons.²⁵ The observation of mixed dimers (**7b-d**) in THF, HMPA/THF, and DMPU/THF and a mixture of mixed dimer **7a** and mixed trimer **9a** in *t*-BuOMe are congruent with previous investigations.

Figure 1 offers insights into both the extent and consequences of mixed aggregation. It is instructive to focus upon three regions of these plots as follows:

(1) The rates for the loss of LDA dimers and formation of mixed aggregates throughout the first 50% conversion are relatively high and nearly equivalent for all solvents. (LDA dimers **3a-d** disappear quickly due to concurrent consumption

(24) The values of $K_{\text{eq(obsd)}}$ listed in Table 2 are crudely approximated by integrating the absorbances of the LDA dimers (3), the mixed dimers (7), and the sum of all resonances corresponding to the homonuclear enolates (2). In the case of *t*-BuOMe, the concentration of mixed aggregates was determined from the sum of the dimer and trimer resonances.

(25) Lucht, B. L.; Collum, D. B., unpublished results.

**Figure 2.**

by the metalation as well as by the formation of mixed dimers **7a-d**.) The earliest portion of the reaction coordinate was investigated under pseudo-first-order conditions as described in the preceding paper. A discussion of the numerous underlying mechanisms will not be repeated here.

(2) The mixed dimers reach maximal concentrations (i.e., $[7]_{\text{max}}$) at approximately 50% conversion (*t*-BuOMe excepted). Semiquantitative analysis of the data depicted in Figure 1 reveals that the promotion of mixed aggregation (eq 2) maintains the following order: *t*-BuOMe > DMPU/THF > HMPA/THF > THF. This appears to correlate neither directly nor inversely with solvent binding constants.^{26,27}

(3) Comparisons of the loss of LDA dimers (**3a-d**) with the loss of the mixed aggregates (**7a-d** and **9a**) in Figure 1 reveal autoinhibitions accompanying mixed aggregate formation. Moreover, these solvent-dependent inhibitions correlate crudely with the solvent-dependent mixed aggregate stabilities (eq 2, Table 2). For example, in THF mixed aggregates form to only a limited extent and the rates slow only modestly in the latter half-lives. At the other extreme, the exceptional stabilization of the mixed aggregates in *t*-BuOMe is accompanied by almost a complete stalling of the metalation at partial conversion.

The autoinhibition can be understood from either of two equivalent perspectives: (a) mixed aggregation depletes the concentration of LDA dimer **3** and, by inference, all species in equilibrium with **3** including the transition structure, or (b) mixed aggregation "stabilizes" the reactant without stabilizing the transition structure (Figure 2). Regardless of perspective, if mixed aggregation is an unproductive side equilibrium in which no new (mixed aggregate-based) reaction pathways emerge, then the rate of the metalation will be inhibited as appears to be the case.

Summary and Conclusions

In the previous paper, we described detailed rate studies of enolizations under conditions that precluded significant effects from mixed aggregation by maintaining pseudo-first-order conditions. These studies revealed that, while the mechanism of enolization proved highly solvent-dependent, the rates were nearly solvent-independent. In this paper we described qualitative NMR spectroscopic investigations of those same enolizations carried to full conversion, conditions that maximize the influence of mixed aggregation. Mixed aggregates do indeed intervene along the reaction coordinate and their influence on the reaction rates is highly solvent-dependent. In some sense, a very simple picture emerges: the solvents that promote the formation of mixed aggregates also cause the reaction to slow considerably as the mixed aggregates appear. The strong

(26) Lucht, B. L.; Collum, D. B. *J. Am. Chem. Soc.* **1995**, *117*, 9863.

(27) Reich, H. J.; Kulicke, K. J. *J. Am. Chem. Soc.* **1996**, *118*, 273.

correlation of the autoinhibition with mixed aggregate stabilities is fully consistent with a model in which contributions from mixed aggregate-based enolization pathways are *not* significant. If so, the mechanisms, more precisely the rate-limiting transition structures, discussed in the preceding paper⁹ are still operative.

As is often the case, however, there are a number of interesting mechanistic subtleties. The most poorly coordinating solvent (*t*-BuOMe) and strongly coordinating solvent (HMPA) both promote mixed aggregation and resulting autoinhibition when compared to solvents of intermediate solvating capacity (THF and DMPU). The solvent-*independent* reactivities of the homonuclear lithium amide dimers and the solvent-*dependent* mixed aggregate stabilities combine to produce overall solvent-*dependent* metalation rates. As discussed previously,²⁸ solvent-dependent reaction rates as measured by k_{rel} or (even worse) by isolated yield provide little mechanistic insight when unsupported by detailed structural and rate studies.

(28) Bernstein, M. P.; Collum, D. B. *J. Am. Chem. Soc.* **1993**, *115*, 8008. Collum, D. B. *Acc. Chem. Res.* **1992**, *25*, 448.

Experimental Section

Detailed discussions of closely related NMR spectroscopic analyses have been described in detail.²⁹ A brief description of these protocols as well as extensive spectroscopic data are archived in the Supporting Information.

Acknowledgment. We acknowledge the National Science Foundation Instrumentation Program (CHE 7904825 and PCM 8018643), the National Institutes of Health (RR02002), and IBM for support of the Cornell Nuclear Magnetic Resonance Facility. We thank the National Institutes of Health for direct support of this work.

Supporting Information Available: ⁶Li, ¹³C, and ¹⁵N NMR spectra (PDF). This material is available free of charge via the Internet at <http://pubs.acs.org>.

JA992063R

(29) Hall, P.; Gilchrist, J. H.; Harrison, A. T.; Fuller, D. J.; Collum, D. B. *J. Am. Chem. Soc.* **1991**, *113*, 9575.